





# Genistein Targets STING-Driven Antiviral Responses

 Tomalika R. Ullah,<sup>a,b</sup> Katherine R. Balka,<sup>c,d</sup> Rebecca L. Ambrose,<sup>a,b</sup> Geneviève Pépin,<sup>a,b,\*</sup> Matthew C. J. Wilce,<sup>d</sup> Jacqueline A. Wilce,<sup>d</sup> Belinda J. Thomas,<sup>a,b,e</sup> Dominic De Nardo,<sup>c,d</sup> Bryan R. G. Williams,<sup>b,f</sup>  Michael P. Gantier<sup>a,b</sup>

<sup>a</sup>Centre for Innate Immunity and Infectious Diseases, Hudson Institute of Medical Research, Clayton, Victoria, Australia

<sup>b</sup>Department of Molecular and Translational Science, Monash University, Clayton, Victoria, Australia

<sup>c</sup>Department of Anatomy and Developmental Biology, Monash Biomedicine Discovery Institute, Monash University, Clayton, Victoria, Australia

<sup>d</sup>Department of Biochemistry and Molecular Biology, Monash Biomedicine Discovery Institute, Monash University, Clayton, Victoria, Australia

<sup>e</sup>Monash Lung and Sleep, Monash Medical Centre, Clayton, Victoria, Australia

<sup>f</sup>Centre for Cancer Research, Hudson Institute of Medical Research, Clayton, Victoria, Australia

**ABSTRACT** Cytoplasmic detection of DNA by cyclic GMP-AMP (cGAMP) synthase (cGAS) is an essential component of antiviral responses. Upon synthesis, cGAMP binds to the stimulator of interferon (IFN) genes (STING) in infected and adjacent cells through intercellular transfer by connexins forming gap-junctions, eliciting a strong IFN- $\beta$ -driven antiviral response. We demonstrate here that Genistein, a flavonoid compound naturally occurring in soy-based foods, inhibits cGAS-STING antiviral signaling at two levels. First, Genistein pretreatment of cGAMP-producing cells inhibited gap-junction intercellular communication, resulting in reduced STING responses in adjacent cells. In addition, Genistein directly blocked STING activation by the murine agonist DMXAA, by decreasing the interaction of STING with TBK1 and IKK $\epsilon$ . As a result, Genistein attenuated STING signaling in human and mouse cells, dampening antiviral activity against Semliki Forest Virus infection. Collectively, our findings identify a previously unrecognized proviral activity of Genistein mediated via its inhibitory effects at two levels of cGAS-STING signaling.

**IMPORTANCE** Several reports suggest that Genistein exhibits antiviral activities against DNA viruses. Our work uncovers a previously unrecognized proviral effect of Genistein, through inhibition of the cGAS-STING pathway at the level of cGAMP transfer and its sensing by STING. This suggests that the use of Genistein as an antiviral should be taken with caution as it may reduce the protective antiviral effects elicited by host STING activation.

**KEYWORDS** Genistein, STING inhibitor, cGAMP, gap junction

Following synthesis by cGAS, cGAMP binding to STING leads to its oligomerisation and interaction with TBK1 and IKK $\epsilon$  kinases (1–3). This results in the phosphorylation of STING and IRF3, promoting a strong antiviral response through IFN- $\beta$  production (2–4). In addition to engaging with STING in infected cells, cGAMP rapidly propagates antiviral responses to uninfected cells through direct extracellular secretion (5), via gap junction intercellular communication (GJIC) (6, 7) or incorporation in viral particles (8).

Naturally occurring small molecules such as flavonoids and flavonoid-like compounds (e.g., Resveratrol) can modulate GJIC (9). Here we initially posited that pharmacological enhancement of GJIC could be used to increase cGAMP-mediated transactivation of adjacent cells and raise antiviral activity. We initially tested a small panel of flavonoid compounds (Genistein, Apigenin, Quercetin, Resveratrol, Kaempferol, and Epigallocatechin gallate [EGCG]) in a coculture model of GJIC. STING-deficient cGAS-overexpressing human cells (HEK-cGAS<sup>low</sup> herein), which make constitutive levels of cGAMP, were cultured together with STING competent mouse L929 cells stably expressing an IFN-sensitive responsive element [ISRE] luciferase reporter, referred to as LL171 herein (6, 10). Pretreatment of the HEK-cGAS<sup>low</sup> cells with the flavonoid compounds potentiated ISRE-luciferase expression, except for Genistein which had an

**Editor** Sabra Klein, Johns Hopkins Bloomberg School of Public Health

**Copyright** © 2022 Ullah et al. This is an open-access article distributed under the terms of the [Creative Commons Attribution 4.0 International license](https://creativecommons.org/licenses/by/4.0/).

Address correspondence to Michael P. Gantier, Michael.gantier@hudson.org.au.

\*Present address: Geneviève Pépin, Department of Medical Biology, Université du Québec à Trois-Rivières, Trois-Rivières, Quebec, Canada.

The authors declare a conflict of interest. Michael Gantier is a named inventor of provisional patents relating to cGAS and STING inhibitors.

This article is a direct contribution from Bryan R.G. Williams, a Fellow of the American Academy of Microbiology, who arranged for and secured reviews by Katherine Fitzgerald, University of Massachusetts Medical School, and Søren Paludan, University of Aarhus, Aarhus, Denmark.

**Received** 19 July 2022

**Accepted** 21 July 2022

**Published** 4 August 2022

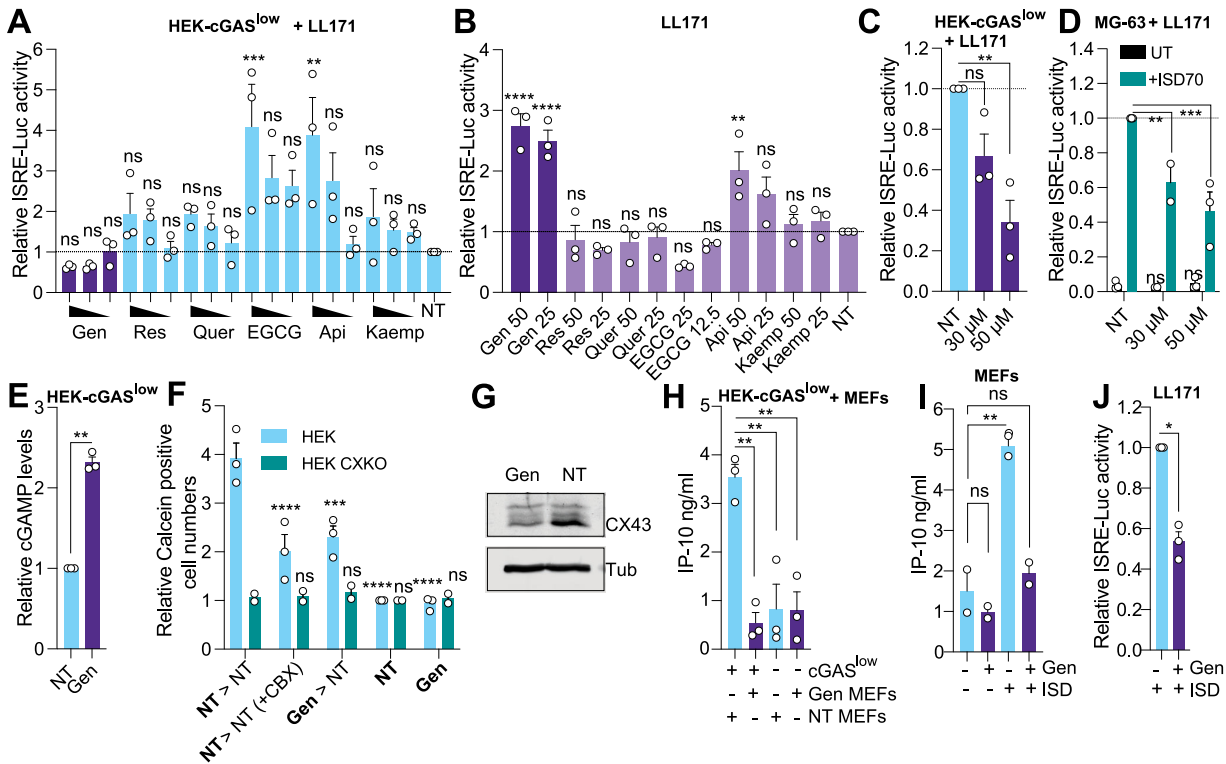


**FIG 1** Genistein inhibits transactivation of neighboring cells. (A) HEK-cGAS<sup>low</sup> cells pretreated with indicated compounds (Genistein [Gen], Resveratrol [Res], Quercetin [Quer], Apigenin [Api], and Kaempferol [Kaemp] at 50, 25, and 12.5 μM; EGCG at 25, 12.5, and 6.25 μM) for 48 h were cocultured overnight with LL171 cells. ISRE-Luciferase levels were measured from the cell lysates the next day. The data are shown relative to nontreated (NT) LL171 cells (*n* = 3). (B) LL171 cells were treated with indicated compounds for 48 h and ISRE-luciferase levels were analyzed. Data are shown relative to NT LL171 cells (*n* = 3). (C) HEK-cGAS<sup>low</sup> cells pretreated with 50 or 30 μM Genistein for 48 h were collected and counted. ~20,000 HEK-cGAS<sup>low</sup> cells were subsequently cocultured overnight with LL171 cells. ISRE-Luciferase levels are shown relative to NT LL171 cells (*n* = 3). (D) MG-63 cells pretreated for 48 h with 30 or 50 μM Genistein were transfected with 2.5 μg/mL of ISD70 for 4 h (after wash to remove ISD70 [7]) or untransfected (UT), and cocultured overnight with the same amount of recipient LL171 cells. ISRE-Luciferase levels are shown relative to the ISD70-treated cells (*n* ≥ 2). (E) HEK-cGAS<sup>low</sup> cells were treated for 48 h with 50 μM Genistein prior to lysis and cGAMP-specific ELISA. Data are shown relative to NT HEK-cGAS<sup>low</sup> cells (*n* = 3). (F) HEK-STING (HEK) and HEK-STING CX KO cells (HEK CXKO) were pretreated with 50 μM Genistein or not (NT) for ~40 h followed by treatment with 2 μg/mL Calcein-AM solution for 1 h. The donor cells (in Bold) were washed, counted, and 7,000 donor cells were cocultured (indicated with ">" sign) with ~40,000 recipient confluent cells of the same genotype, in the presence or not of CBX (100 μM). Calcein dye transfer was quantified after 4 h by counting the number of Calcein positive cells per fields. Data are shown reported to NT condition [Calcein positive cells only] (*n* = 2 for HEK CXKO and *n* = 3 for HEK). (G) Western blot analysis of CX43 levels from the lysates of MEFs treated with 50 μM Genistein for 48 h (representative of *n* = 2). (H) MEFs pretreated with or without 50 μM Genistein for ~40 h were cocultured overnight with HEK-cGAS<sup>low</sup> (cGAS<sup>low</sup>) cells. Supernatants were collected, and mouse IP-10 levels measured by specific ELISA (*n* = 3). (I) MEFs were pretreated for 48 h with 50 μM Genistein prior to the overnight transfection with 1 μg/mL ISD45 and mouse IP-10 levels measurement by specific ELISA (*n* = 2). (J) LL171 cells were pretreated for 1 h with 40 μM Genistein, prior to transfection with 2.5 μg/mL ISD45 for 6 h. ISRE-Luciferase levels are shown relative to the ISD-treated cells (*n* = 3). (A, B, C, D, E, F, H, I, J) Each point represents the mean data for each independent experiment. Unpaired t-tests (E, J), two-way (D, F) or one-way (A, B, C, H, I) ANOVA comparisons are shown. Data are mean ± s.e.m.; \*\*, *P* ≤ 0.01; \*\*\*, *P* ≤ 0.001; \*\*\*\*, *P* ≤ 0.0001; ns, nonsignificant.

inhibitory effect (Fig. 1A). Conversely, Genistein direct treatment of LL171 cells rather induced ISRE-luciferase expression (Fig. 1B). Although not exhibiting any visible toxicity on the HEK-cGAS<sup>low</sup> cells at the doses used, Genistein treatment reduced cell proliferation above 30 μM (Fig. S1A). To circumvent this, we normalized the number of cGAMP-producing cells after Genistein treatment and confirmed a dose-dependent inhibition of cGAMP transactivation of cocultured LL171 cells by Genistein (Fig. 1C). Similarly, pretreatment of connexin (CX) expressing human MG-63 cells with Genistein (11), that were subsequently transfected with an immunostimulatory DNA (ISD) to activate cGAS (12), significantly decreased ISRE-luciferase expression from cocultured LL171 cells (Fig. 1D). It is noteworthy that intracellular levels of cGAMP were increased by Genistein in HEK cGAS<sup>low</sup> cells (Fig. 1E), indicating an inhibition of GJIC aligned with the accumulating cGAMP levels observed. Accordingly, GJIC-dependent transfer of the small molecular weight dye Calcein was decreased when the Calcein-loaded HEK donor cells had previously been treated with Genistein (Fig. 1F). Genistein inhibition of Calcein transfer was seen in HEK-STING cells naturally expressing connexin (CX) 43 and 45 (HEK-STING herein) (6) and was comparable to that obtained with carbenoxolone (CBX), a known inhibitor

of connexin-forming gap junctions (6, 7) (Fig. 1F). However, HEK-STING CX43/45 double knock-out cells (HEK-STING CX KO herein) failed to show any Calcein transfer, suggesting an effect of Genistein at the level of CX43/45 (Fig. 1F). In agreement with this concept, Genistein treatment of SV40T immortalized mouse embryonic fibroblasts (MEFs) significantly decreased CX43 levels by ~60%, as measured by Western blotting (CX43 was undetectable in HEK cells with this method) (Fig. 1G and Fig. S1B).

Gap junctions are formed by two connexin-forming hemichannels, with one contributed by each adjacent cell to ensure intercellular communication of cGAMP (6, 10). Surprisingly, Genistein pretreatment of the MEFs entirely ablated the transactivation from the cocultured HEK-cGAS<sup>low</sup> cells, measured by the secretion of mouse IP-10 (Fig. 1H). This strong inhibitory effect was unexpected given that pretreatment of donor cGAMP-producing HEK-cGAS<sup>low</sup> cells only partially decreased transactivation of the recipient cells (Fig. 1C). Critically, pretreatment of the MEFs or LL171 cells significantly blunted IP-10 production or ISRE-luciferase expression upon ISD transfection (Fig. 1I and J) suggesting a direct inhibition of STING sensing independent of CX inhibition.

In agreement with this, we observed a dose-dependent inhibitory activity of Genistein on ISRE-Luciferase in LL171 cells stimulated with the murine STING agonist DMXAA (Fig. 2A). To better define how Genistein impacts STING downstream signaling upon activation, we assessed its activity on NF- $\kappa$ B-Luciferase and IFN- $\beta$ -Luciferase levels in HEK-STING cells that make endogenous cGAMP upon overexpression of cGAS-GFP (7, 13). Genistein inhibited both branches of STING signaling equivalently (Fig. 2B), indicating that its effect was mediated upstream of IRF3 and NF- $\kappa$ B. Western blot analysis of Genistein pretreated immortalized mouse bone marrow-derived macrophages (iBMDMs) stimulated with DMXAA showed a 40 to 50% decrease of STING phosphorylation, and, to a lesser degree, IKK $\epsilon$  and TBK1, which resulted in decreased IRF3 (most visible at 1 h) and p65 phosphorylation (most visible at 2 h) (Fig. 2C and Fig. S1C). This was concurrent with a significant decrease of TNF- $\alpha$  production by the iBMDMs (Fig. 2D). Critically, Genistein pretreatment also strongly reduced IP-10 production by human monocytic THP-1 cells stimulated with a cGAMP analog (ADU-S100) or a synthetic STING agonist (diABZI) (14) (Fig. 2E)—the latter observation being replicated in MG-63 cells (Fig. 2F). Genistein also reduced IFN- $\beta$ -Luciferase driven by overexpression of a gain of function STING variant R284S (1, 15) (Fig. 2G).

Mechanistically, Genistein's inhibitory activity is not targeted at the level of STING trafficking as evidenced by the unaltered formation of STING foci in HEK-STING cells following stimulation with diABZI (Fig. S2A). Similarly, Genistein did not decrease IFN- $\beta$ -Luciferase driven by overexpression of human TBK1 or IKK $\epsilon$  (Fig. 2H). Nonetheless, Genistein decreased the interaction of mCitrine tagged STING with phospho-TBK1 and IKK $\epsilon$  following stimulation of iBMDMs with DMXAA and pull-down of mCitrine-STING (Fig. 2I). This suggests that Genistein limits STING signaling through the modulation of the STING/TBK1/IKK $\epsilon$  interactions, presumably through its interaction with STING since it did not affect signaling driven by overexpression of human TBK1 or IKK $\epsilon$ . Accordingly, *in silico* molecular docking of Genistein with STING identified 3 locations where Genistein was predicted to bind. We obtained 9 binding poses of interaction, and that with the lowest binding energy score, located in proximity to the STING C-terminal tail required for TBK1 recruitment (16), is shown in Fig. 2J and in Fig. S3. This illustrates the potential for a direct interaction of Genistein with STING. Albeit warranting further validation, these results collectively suggest that Genistein impacts STING signaling by direct targeting and preventing its interaction with TBK1/IKK $\epsilon$ . It is also noteworthy that beyond its effect on STING signaling, Genistein also decreased IFN- $\beta$ -Luciferase upon TLR3 activation, presumably due to its inhibitory effect on NF- $\kappa$ B activity (17) (Fig. S2B).

Finally, to determine whether the inhibitory effect of Genistein on STING signaling sensitized cells to viral infections, we tested whether it was able to block the antiviral activity of the STING agonist DMXAA. While DMXAA priming of LL171 cells promoted a strong antiviral effect against infection by the RNA Semliki Forest Virus (SFV), pretreatment with Genistein prior to DMXAA reduced this antiviral effect (Fig. 2K and Fig. S4A, S4B). This proviral effect of Genistein was comparable to that obtained with anti-IFNAR1 antibody treatment. Accordingly, the combination of Genistein with the anti-IFNAR1 antibody did not result in a robust increase of viral

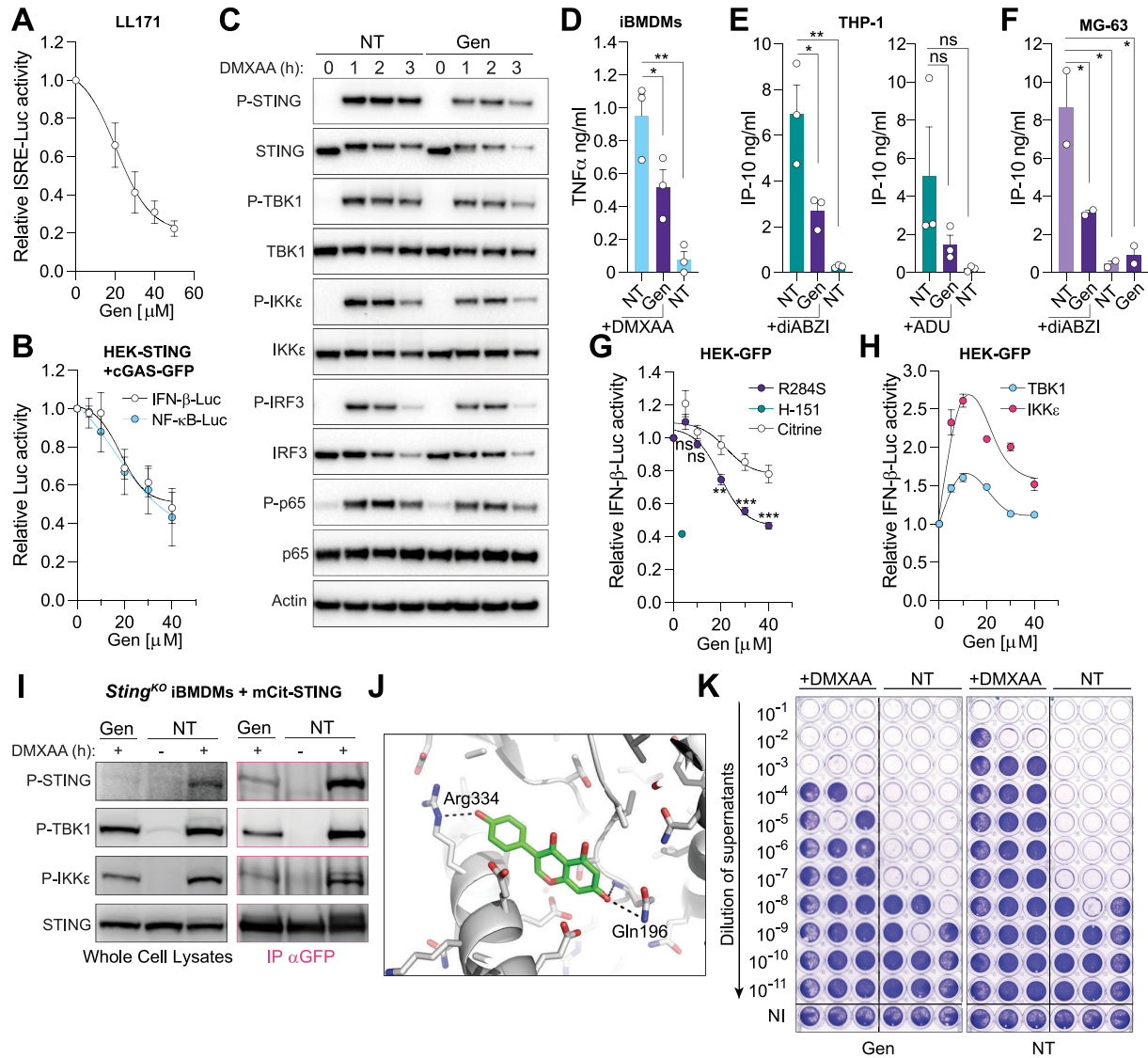


**FIG 2** Genistein inhibits STING sensing of its ligands. (A) LL171 cells were treated for 1 h with indicated dose of Genistein followed by DMXAA stimulation (20  $\mu\text{g}/\text{mL}$ ) for  $\sim 8$  h. ISRE-luciferase levels were normalized to the “DMXAA only” condition, after background correction with NT condition ( $n = 4$ ). (B) HEK-STING cells transiently overexpressing cGAS-GFP, and an IFN- $\beta$ -luciferase or an NF- $\kappa$ B-luciferase reporter were treated overnight with indicated dose of Genistein. The data are shown reported to the “NT” condition ( $n = 3$  for IFN- $\beta$ -luciferase and  $n = 2$  for NF- $\kappa$ B-luciferase). (C) iBMDMs were pretreated or not for 1 h with 40  $\mu\text{M}$  Genistein, washed and treated with 50  $\mu\text{g}/\text{mL}$  DMXAA for indicated times before lysis and immunoblotting ( $n = 3$ ). (D) iBMDM cells were pretreated or not for 1 h with 40  $\mu\text{M}$  Genistein prior to overnight stimulation with 50  $\mu\text{g}/\text{mL}$  DMXAA and mouse TNF- $\alpha$  levels measured by specific ELISA ( $n = 3$ ). (E) Undifferentiated THP-1 cells were pretreated or not for 1 h with 40  $\mu\text{M}$  Genistein before 6 h stimulation with 100 nM diABZI (left) or 30  $\mu\text{M}$  ADU-S100 (right), and IP-10 levels were analyzed by specific ELISA ( $n = 3$ ). (F) MG-63 cells were pretreated or not for 1 h with 40  $\mu\text{M}$  Genistein, followed by 7 h stimulation with 100 nM diABZI, and IP-10 levels were analyzed by specific ELISA ( $n = 2$ ). (G, H) HEK293T-GFP (HEK-GFP) transiently expressing an IFN- $\beta$ -luciferase reporter with either Citrine (control), STING(R284S) (G), TBK1, or IKK $\epsilon$  vectors (H), were treated overnight with indicated dose of Genistein or 3.6  $\mu\text{M}$  H-151 (STING inhibitor). Data are shown relative to the “NT” condition ( $n = 3$ ). (I) Immunoblot of *Sting*<sup>KO</sup> iBMDMs expressing mCitrine-STING, after 1 h stimulation with 50  $\mu\text{g}/\text{mL}$  DMXAA and 150  $\mu\text{M}$  Genistein. Pink: pull-down of mCitrine-STING with anti-GFP antibody. Black: whole cell lysates ( $n = 3$ ). (J) *In silico* docking of Genistein with a STING dimer—the model shown is that of pose 1, with the most favorable binding whole (see Text S1 and Fig. S3). Genistein is shown as sticks and 3 h-bonds are indicated as dashed lines. (K) LL171 cells were pretreated for 1 h with or without 40  $\mu\text{M}$  Genistein followed by stimulation with 20  $\mu\text{g}/\text{mL}$  DMXAA. After 4 h stimulation with DMXAA, the cells were washed and infected in biological triplicate with Semliki Forest virus (SFV) for 24 h (MOI 2). Viral titers were assayed with log<sub>10</sub> fold dilutions on confluent Vero cells as shown. NI: not infected (uninfected cells stain with crystal violet); NT: nontreated prior infection. Data shown are representative of three independent experiments. (D, E, F) Each point represents the mean data for each independent experiment. Two-way (G) or one-way (D, E, F) ANOVA comparisons are shown. Data are mean  $\pm$  s.e.m.; \*,  $P \leq 0.05$ ; \*\*,  $P \leq 0.01$ ; \*\*\*,  $P \leq 0.001$ ; ns, is nonsignificant.

replication (Fig. S4B). This supports the predominant proviral effects of Genistein seen in this system as relying on type-I IFN inhibition. However, we note that Genistein modestly increased the proviral effect of the anti-IFNAR1 antibody, presumably due to its inhibitory impact on NF- $\kappa$ B activity (17) (Fig. S4B).

Our findings collectively establish the proviral activity of Genistein through its inhibition of the cGAS-cGAMP-STING pathway at two levels. On one hand, Genistein can block the transfer of cGAMP to adjacent cells, through the reduction of GJIC. This diminishes the amplification of antiviral responses mediated by cGAMP intercellular transfer (6, 7). Mechanistically, our data in MEFs suggest that this effect is driven by a decrease in CX43 mediated by Genistein. However, cGAMP can also be transferred between cells through hemichannels formed by CX26, CX31, CX32, CX40 and CX62 (6). Therefore, it remains to be determined whether hemichannels beyond those involving CX43 are also targeted by Genistein. On the other hand, Genistein has been shown to directly inhibit STING activation by its agonists (18), which we posit results from a direct interaction of Genistein with STING, thereby impeding its interaction with TBK1 and IKK $\epsilon$ . However, further studies will be required to ascertain whether this activity of Genistein also modulates STING-driven autophagy and apoptosis. We also showed that Genistein has a small effect on TLR3-driven antiviral responses suggesting it may have broad immunosuppressive effects on IFN- $\beta$  production beyond STING. Importantly, Genistein has been shown to have protective effects in several animal models of diseases that have now been linked to STING signaling (19), including acute pancreatitis (20), DMBA-induced cancer (21), nonalcoholic fatty liver and alcoholic liver diseases (22, 23).

Several studies have previously reported an antiviral effect of Genistein against DNA viruses such as HSV-1, cytomegalovirus, or Herpes B Virus, leading to the proposition that its topical administration could be a promising antiviral treatment against these viruses (24). Our findings suggest that its inhibitory effects on type-I IFN responses could confound other antiviral activities in the context of DNA viruses that naturally engage this pathway, prompting caution in its therapeutic development as an antiviral.

**Data availability.** Additional numerical data used to generate published graphs that support the findings of this study are available on request from the corresponding author.

## SUPPLEMENTAL MATERIAL

Supplemental material is available online only.

**TEXT S1**, PDF file, 0.1 MB.

**FIG S1**, PDF file, 0.1 MB.

**FIG S2**, PDF file, 0.1 MB.

**FIG S3**, PDF file, 0.6 MB.

**FIG S4**, PDF file, 0.4 MB.

## ACKNOWLEDGMENTS

We thank V. Hornung for the cGAS-GFP expressing vector, HEK-cGAS<sup>low</sup>, HEK-STING, and HEK-STING CX43/45<sup>-/-</sup> cells; A. Mansell for TBK1 and IKK $\epsilon$  vectors; K. Fitzgerald for the pLuc-IFN- $\beta$  reporter; M. Pelegrin for LL171 cells; and N.A. de Weerd and A. Matthews for the MAR1-5A3 antibody.

This work was supported by the Australian National Health and Medical Research Council (1124485 to M.P.G.); the Australian Research Council (140100594 Future Fellowship to M.P.G.); the Quebec Fonds de Recherche du Québec (FRSQ)–Santé (35071 to G.P.); and the Victorian Government's Operational Infrastructure Support Program.

## REFERENCES

- Balka KR, Louis C, Saunders TL, Smith AM, Calleja DJ, D'Silva DB, Moghaddas F, Tailler M, Lawlor KE, Zhan Y, Burns CJ, Wicks IP, Miner JJ, Kile BT, Masters SL, De Nardo D. 2020. TBK1 and IKK $\epsilon$  act redundantly to mediate STING-induced NF- $\kappa$ B responses in myeloid cells. *Cell Rep* 31:107492. <https://doi.org/10.1016/j.celrep.2020.03.056>.
- Liu S, Cai X, Wu J, Cong Q, Chen X, Li T, Du F, Ren J, Wu YT, Grishin NV, Chen ZJ. 2015. Phosphorylation of innate immune adaptor proteins MAVS, STING, and TRIF induces IRF3 activation. *Science* 347:aaa2630. <https://doi.org/10.1126/science.aaa2630>.
- Zhao B, Du F, Xu P, Shu C, Sankaran B, Bell SL, Liu M, Lei Y, Gao X, Fu X, Zhu F, Liu Y, Laganowsky A, Zheng X, Ji J-Y, West AP, Watson RO, Li P. 2019. A conserved PLPLRT/SD motif of STING mediates the recruitment and activation of TBK1. *Nature* 569:718–722. <https://doi.org/10.1038/s41586-019-1228-x>.
- Sun L, Wu J, Du F, Chen X, Chen ZJ. 2013. Cyclic GMP-AMP synthase is a cytosolic DNA sensor that activates the type I interferon pathway. *Science* 339:786–791. <https://doi.org/10.1126/science.1232458>.
- Lahey LJ, Mardjuki RE, Wen X, Hess GT, Ritchie C, Carozza JA, Böhnert V, Maduke M, Bassik MC, Li L. 2020. LRR8A:C/E heteromeric channels are ubiquitous transporters of cGAMP. *Mol Cell* 80:578–591.e575. <https://doi.org/10.1016/j.molcel.2020.10.021>.
- Ablasser A, Schmid-Burgk JL, Hemmerling I, Horvath GL, Schmidt T, Latz E, Hornung V. 2013. Cell intrinsic immunity spreads to bystander cells via the intercellular transfer of cGAMP. *Nature* 503:530–534. <https://doi.org/10.1038/nature12640>.
- Pépin G, De Nardo D, Rootes CL, Ullah TR, Al-Asmari SS, Balka KR, Li H-M, Quinn KM, Moghaddas F, Chappaz S, Kile BT, Morand EF, Masters SL, Stewart

- CR, Williams BRG, Gantier MP, Horner SM, Gale M, Silverman R. 2020. Connexin-dependent transfer of cGAMP to phagocytes modulates antiviral responses. *mBio* 11 <https://doi.org/10.1128/mBio.03187-19>.
8. Bridgeman A, Maelfait J, Davenne T, Partridge T, Peng Y, Mayer A, Dong T, Kaever V, Borrow P, Rehwinkel J. 2015. Viruses transfer the antiviral second messenger cGAMP between cells. *Science* 349:1228–1232. <https://doi.org/10.1126/science.aab3632>.
  9. Aasen T, Mesnil M, Naus CC, Lampe PD, Laird DW. 2016. Gap junctions and cancer: communicating for 50 years. *Nat Rev Cancer* 16:775–788. <https://doi.org/10.1038/nrc.2016.105>.
  10. Pépin G, Nejad C, Thomas BJ, Ferrand J, McArthur K, Bardin PG, Williams BRG, Gantier MP. 2017. Activation of cGAS-dependent antiviral responses by DNA intercalating agents. *Nucleic Acids Res* 45:198–205. <https://doi.org/10.1093/nar/gkw878>.
  11. Polusani SR, Kar R, Riquelme MA, Masters BS, Panda SP. 2011. Regulation of gap junction function and Connexin 43 expression by cytochrome P450 oxidoreductase (CYPOR). *Biochem Biophys Res Commun* 411:490–495. <https://doi.org/10.1016/j.bbrc.2011.06.132>.
  12. Valentin R, Wong C, Alharbi AS, Pradeloux S, Morros MP, Lennox KA, Ellyard JJ, Garcin AJ, Ullah TR, Kusuma GD, Pépin G, Li H-M, Pearson JS, Ferrand J, Lim R, Veedu RN, Morand EF, Vinuesa CG, Behlke MA, Gantier MP. 2021. Sequence-dependent inhibition of cGAS and TLR9 DNA sensing by 2'-O-methyl gapmer oligonucleotides. *Nucleic Acids Res* 49:6082–6099. <https://doi.org/10.1093/nar/gkab451>.
  13. Haag SM, Gulen MF, Reymond L, Gibelin A, Abrami L, Decout A, Heymann M, van der Goot FG, Turcatti G, Behrendt R, Ablasser A. 2018. Targeting STING with covalent small-molecule inhibitors. *Nature* 559:269–273. <https://doi.org/10.1038/s41586-018-0287-8>.
  14. Ramanjulu JM, Pesiridis GS, Yang J, Concha N, Singhaus R, Zhang S-Y, Tran J-L, Moore P, Lehmann S, Eberl HC, Muelbauer M, Schneck JL, Clemens J, Adam M, Mehlmann J, Romano J, Morales A, Kang J, Leister L, Graybill TL, Charnley AK, Ye G, Nevins N, Behnia K, Wolf AI, Kasparcova V, Nurse K, Wang L, Puhl AC, Li Y, Klein M, Hopson CB, Guss J, Bantscheff M, Bergamini G, Reilly MA, Lian Y, Duffy KJ, Adams J, Foley KP, Gough PJ, Marquis RW, Smothers J, Hoos A, Bertin J. 2018. Design of amidobenzimidazole STING receptor agonists with systemic activity. *Nature* 564:439–443. <https://doi.org/10.1038/s41586-018-0705-y>.
  15. Saldanha RG, Balka KR, Davidson S, Wainstein BK, Wong M, Macintosh R, Loo CKC, Weber MA, Kamath V, Moghaddas F, De Nardo D, Gray PE, Masters SL, AADRY. 2018. A mutation outside the dimerization domain causing atypical STING-associated vasculopathy with onset in infancy. *Front Immunol* 9:1535. <https://doi.org/10.3389/fimmu.2018.01535>.
  16. Zhang C, Shang G, Gui X, Zhang X, Bai X-c, Chen ZJ. 2019. Structural basis of STING binding with and phosphorylation by TBK1. *Nature* 567:394–398. <https://doi.org/10.1038/s41586-019-1000-2>.
  17. Davis JN, Kucuk O, Sarkar FH. 1999. Genistein inhibits NF- $\kappa$ B activation in prostate cancer cells. *Nutr Cancer* 35:167–174. [https://doi.org/10.1207/S15327914NC352\\_11](https://doi.org/10.1207/S15327914NC352_11).
  18. Wang C, Wang X, Velepparambil M, Kessler PM, Willard B, Chattopadhyay S, Sen GC. 2020. EGFR-mediated tyrosine phosphorylation of STING determines its trafficking route and cellular innate immunity functions. *EMBO J* 39 <https://doi.org/10.15252/embj.2019104106>.
  19. Ablasser A, Chen ZJ. 2019. cGAS in action: expanding roles in immunity and inflammation. *Science* 363 <https://doi.org/10.1126/science.aat8657>.
  20. Xia S, Wang J, Kalionis B, Zhang W, Zhao Y. 2019. Genistein protects against acute pancreatitis via activation of an apoptotic pathway mediated through endoplasmic reticulum stress in rats. *Biochem Biophys Res Commun* 509:421–428. <https://doi.org/10.1016/j.bbrc.2018.12.108>.
  21. Wei H, Bowen R, Zhang X, Lebwohl M. 1998. Isoflavone genistein inhibits the initiation and promotion of two-stage skin carcinogenesis in mice. *Carcinogenesis* 19:1509–1514. <https://doi.org/10.1093/carcin/19.8.1509>.
  22. Zhao L, Wang Y, Liu J, Wang K, Guo X, Ji B, Wu W, Zhou F. 2016. Protective effects of Genistein and Puerarin against chronic alcohol-induced liver injury in mice via antioxidant, anti-inflammatory, and anti-apoptotic mechanisms. *J Agric Food Chem* 64:7291–7297. <https://doi.org/10.1021/acs.jafc.6b02907>.
  23. Xin X, Chen C, Hu YY, Feng Q. 2019. Protective effect of genistein on non-alcoholic fatty liver disease (NAFLD). *Biomed Pharmacother* 117:109047. <https://doi.org/10.1016/j.biopha.2019.109047>.
  24. LeCher JC, Diep N, Krug PW, Hilliard JK. 2019. Genistein has antiviral activity against Herpes B virus and acts synergistically with antiviral treatments to reduce effective dose. *Viruses* 11:499. <https://doi.org/10.3390/v11060499>.